2007 IEEE International Conference on
Robotics and Automation
Roma, Italy, 10-14 April 2007

Simplectic Architectures for True Multi-axial Accelerometers: A Novel Application of Parallel Robots

Philippe Cardou and Jorge Angeles, IEEE Fellow

Abstract— **Several triaxial accelerometers are known. However, to the knowledge of the authors, no *true*, triaxial accelerometers are commercially available. By *true* we mean an accelerometer which would pick up the three components of point-accelerations using one single proof-mass. What we propose is novel architecture classes of parallel-kinematics-machine for multi-axial accelerometers, that is, accelerometers that can measure n components of point-accelerations, where $n = 1, 2, 3$. We call these architectures *simplectic*, as they use $n + 1$ legs oriented normally to the $n + 1$ faces of the regular simplex associated with the n-dimensional subspace of measured acceleration components. We show that the simplectic biaxial accelerometer can be fabricated using micromachining MEMS techniques, while the simplectic triaxial accelerometer lends itself to compliant-mechanism fabrication techniques. CAD models of the prototypes proposed are provided for all of the three novel mechanical architectures proposed. Finally, the direct kinematics problems associated with the simplectic biaxial and triaxial accelerometers are shown to be linear in both cases. This feature simplifies the estimation of the proof-mass displacement from piezoresistive or piezoelectric measurements taken at the flexible joints connecting the legs of the mechanism to the rigid body whose acceleration is under estimation.**

I. INTRODUCTION

Inertial Navigation Systems (INS) offer many advantages over other navigation systems:

1) They do not depend on any external reference, which makes them highly reliable;
2) they can be produced in relatively compact sizes, thanks to MEMS fabrication processes;
3) they are relatively cheap;
4) they are energy-efficient; and
5) they offer a large bandwidth.

However, the computation of the state variables used in navigation from the readouts of Inertial Measurement Units (IMUs)—acceleration, angular acceleration, angular velocity, or a combination thereof—requires time-integration, which renders any algorithm unstable. The reason behind is the unavoidable bias errors in the measurements, in light of the inherent integrator instability—the integrator poles are all zero. Nevertheless, INS give good results when coupled with external aids such as GPS [1], [2]. Indeed, INS and GPS are good complements to each other, as GPS give stable position information with relatively low resolution and low frequency, while INS operate at high frequencies and have a high resolution on acceleration and angular velocity. Moreover, INS allow the vehicle to operate in case of a temporary loss of the GPS signal during certain lapses. The level of autonomy provided by INS is thus highly dependent on the bias errors embedded in their inertial measurements.

The need for inertial sensors with high resolution and low bias error is thus apparent. Low noise-to-signal ratio is also important for the instrument to keep a good bandwidth, and, therefore, offer a significant advantage over GPS. These two characteristics can be enhanced by increasing the mass used to generate the inertia force [3]. MEMS have the advantage of being compact and cheap, but they are limited with regard to the size and the density of their suspended mass. In addition, they confine the designer to elementary mechanical architectures, which often render the system sensitive to other motion variables than the ones of interest. As an example of this, we have cross-axis sensitivity when an accelerometer signal is influenced by the acceleration components that are perpendicular to the sensitive axis.

The vast majority of commercially available accelerometers function on the principle of mass-spring systems. The mass, which is referred to as the proof mass, is suspended on the accelerometer frame by one or several flexible beams, which act as the springs. In general, the mechanical system is designed so that the proof mass can only translate along one, two, or three independent directions, which we will call its *sensitive axes*. Hence, when the accelerometer frame is subjected to an acceleration input that is parallel to the sensitive axis, the proof mass induces a proportional deflection of its supporting beams. The resulting proof-mass displacements can then be measured, thus yielding an estimate of one, two, or three components of the acceleration of the accelerometer frame.

To the knowledge of the authors, triaxial accelerometers currently available on the market are layouts of three uniaxial accelerometers that measure acceleration components in orthogonal directions not of one, but of three distinct points of a rigid body. Prototypes of *true* triaxial accelerometers, i.e., accelerometers that use the same proof mass to measure all three components of the acceleration of one single point, have been produced in the past. The accelerometers reported in [4]–[7] are micromachined; all work under the

Philippe Cardou is a Ph.D. candidate at the Department of Mechanical Engineering, McGill University, Room 352, 817 Sherbrooke St. W., Montreal, QC, H3A 2K6, Canada pcardou@cim.mcgill.ca

Jorge Angeles is a Professor at the Department of Mechanical Engineering, McGill University, Room 352, 817 Sherbrooke St. W., Montreal, QC, H3A 2K6, Canada angeles@cim.mcgill.ca

Both authors are affiliated with the Centre for Intelligent Machines of McGill University.

1-4244-0602-1/07/$20.00 ©2007 IEEE.

same principle illustrated in Fig. 1. In these accelerometers,

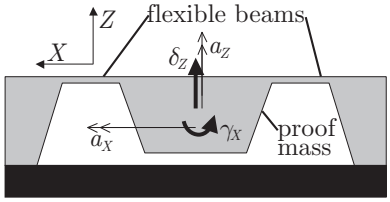

Fig. 1. Working principle of existing compliant *true* triaxial accelerometers

the proof-mass center of gravity is lower than the beam anchors. Therefore, any acceleration a_X in the X-axis direction results in a proof-mass angular displacement γ_X. Conversely, accelerations a_Z directed along the Z-axis induce a proof-mass displacement δ_Z in the same direction. The proof-mass displacements can be estimated by means of piezoresistive sensors on the flexible beams or by means of capacitance variations between the bottom surface of the proof-mass and the handle wafer displayed in black in Fig. 1. However, due to the unidirectional nature of the etching processes used in micromachining, all of these accelerometers have anisotropic mechanical structures, which make them sensitive to parasitic angular acceleration effects. These accelerometers may be labelled *compliant* true triaxial accelerometers, as opposed to another type of true triaxial accelerometers [8] in which the proof-mass is levitated electrostatically. Since the *electrostatic* true triaxial accelerometers are not in the same price range—nor in the same energy consumption range—as the common compliant accelerometers, their mode of operation will not be further described in this paper.

What we propose is mechanisms with the architectures of parallel-kinematics machines (PKMs), allowing the measurement of one, two or three of the acceleration components of one single point of a rigid body. The biaxial accelerometer architecture is intended for microfabrication in single-crystal silicon, whereas the uni- and triaxial accelerometer architectures are intended for millimeter-scale fabrication in polyurethane.

II. The Novel Architectures

In general, an accelerometer comprises a *proof-mass* $\mathcal{M}$ and a *suspension* coupling the mass with the *accelerometer frame*. The latter is rigidly mounted onto the moving body whose position, velocity and acceleration are to be measured.

The novelty of the accelerometers introduced here lies in their versatile architecture. Versatility means that, with a common feature of their architecture, the accelerometers allow for the measurement of one, two and three acceleration components. The novel architecture can be termed *simplectic* in that the suspension consists of $n+1$ *legs*, where n is the number of acceleration components that the accelerometer is capable of measuring. Here, we recall that a *simplex*, in the realm of mathematical programming [9], is a polyhedron with the minimum number of vertices embedded in $\mathbb{R}^n$. Therefore, in one-dimensional space, the simplex is a line segment, its two "vertices" being its two end-points; in two-dimensional space, the simplex is a triangle; in three-dimensional space, a tetrahedron. While the shapes of the triangle and the tetrahedron can, in principle, be arbitrary, one common feature of our accelerometer class is that the triangle is equilateral and the tetrahedron is regular. The outcome is that the accelerometer is equally sensitive in all directions of motion, which makes these architectures *isotropic*. Here, we prefer to speak of *isotropy* rather than *symmetry*, as the latter, including the former as special instance, is more general. Indeed, in the case of accelerometers, having an isotropic architecture implies that the dynamic properties of the sensor are the same in all directions. Moreover, the $n+1$ legs provide *redundancy* in the measurements, thereby providing *robustness* against measurement errors. We describe below the three types of accelerometers, for $n = 1, 2$ and 3, in this order.

The rationale behind the design principle used in all three accelerometer types lies in the mobility analysis of kinematic chains, as first proposed in [10] and then applied systematically in [11] to the design of parallel manipulators. Furthermore, the building block of the three accelerometer types is the Π-joint[1], as described in detail in [11], and recalled presently in Section III. The Π-joint lends itself to implementation using either MEMS technology or a compliant mechanism, whereby the links and joints are all fabricated of one single piece, as proposed in [13].

A. The 2ΠΠΠ Uniaxial Accelerometer Architecture

The one-dimensional accelerometer is intended to measure the acceleration of a point constrained to move along a line. This is achieved by means of a ΠΠ leg-architecture. A Π joint is, essentially, a parallelogram linkage. In order to obtain a one-dimensional design, we use two opposing ΠΠ legs lying in perpendicular planes to sustain the proof-mass, as shown in Fig. 2. This architecture allows only motion

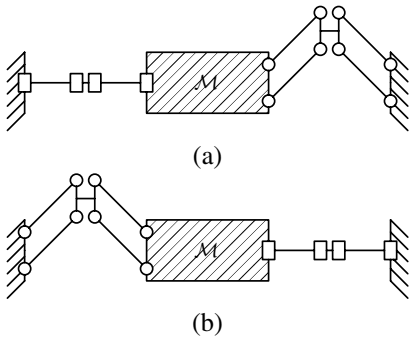

Fig. 2. The uniaxial 2ΠΠ accelerometer: (a) top view; (b) front view.

along the line of intersection of the two planes containing

[1] Π stands for "Pi"-joint, as termed by Hervé [12].

the Π joints, while providing a high stiffness in a plane normal to this direction. For Earth-bound applications, the accelerometer may be oriented so that each of the two orthogonal planes containing the legs forms a 45° angle with respect to the vertical, thereby eliminating virtually any parasitical displacements produced by gravity.

B. The $3\Pi\Pi\Pi$ *Biaxial Accelerometer Architecture*

Other compliant planar parallel mechanisms have been proposed in the past, among which we may cite the one proposed by Yi et al. [14]. These researchers produced a compliant version of the planar 3RRR parallel mechanism. In our case, however, we are to achieve translations in the plane only; hence, we start from a linkage which constrains any proof mass rotation. By laying out the three $\Pi\Pi\Pi$ legs in a common plane at 120° from one another, that is, along the three medians of an equilateral triangle, we obtain the mechanism shown in Fig. 3. This mechanism allows translation in the common plane, while providing a high stiffness in a direction normal to the plane.

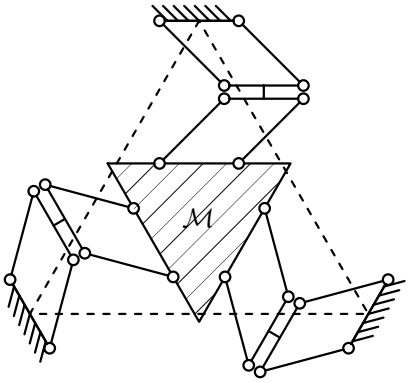

Fig. 3. The biaxial $3\Pi\Pi\Pi$ accelerometer

C. The $4R\Pi\Pi\Pi R$ *Triaxial Accelerometer Architecture*

Many a parallel-robot architecture is available to generate pure translations of the moving platform with respect to the base, e.g. [15] and [16]. We may also cite the compliant parallel mechanism of [17], which allows for pure translations of its moving platform in space. Our device is based on a novel architecture made up of the "legs" of the Japan Mechanical Engineering Laboratory (MEL) Micro Finger [13].

The proposed architecture is shown in Fig. 4, with a regular, heavy tetrahedron $\mathcal{M}$ playing the role of the moving platform, used as the proof-mass of the accelerometer. The four "legs" of the device are attached, at one end, to the tetrahedron-shaped proof-mass $\mathcal{M}$, at the other end to the moving body on which the accelerometer is mounted. This body is the accelerometer frame. Each leg is a $R\Pi\Pi\Pi R$ chain, where R stands for revolute, or pin joint. The $R\Pi\Pi\Pi R$ chain includes two revolute joints, one at each of its two

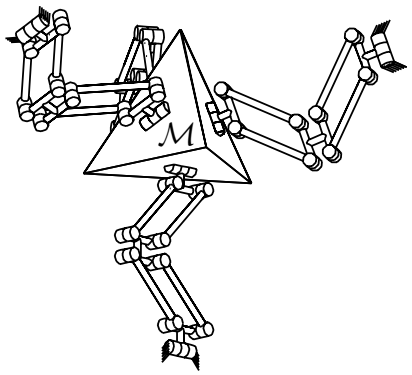

Fig. 4. The triaxial $4R\Pi\Pi\Pi R$ accelerometer

ends, coupling the leg to the tetrahedron and to the body[2]. These two revolutes have their axes parallel to a line passing through the vertex of each triangular face of the tetrahedron and normal to the opposite edge. Moreover, the midplanes of the two parallelogram linkages are coincident and contain the two R-joint axes. We refer to the layout of Fig. 4 as the $4R\Pi\Pi\Pi R$-mechanism, for it consists of four $R\Pi\Pi\Pi R$ legs. To ensure *full mechanical isotropy*[3] , these legs are placed to form a regular tetrahedron. Notice that the mechanism thus resulting comprises 40 flexures distributed onto four legs, whereas the architecture proposed in [17] was made up of 51 flexures in three legs.

III. The Compliant Realizations

The common compliant approximation of a revolute joint is a straight flexible beam cast at both ends. If two such beams are identical and connected to the same two rigid bodies in such a way that their flexible directions given by the (parallel) axes about which the rigid cross-sections rotate are parallel, then the mechanism formed thereby can be called a compliant Π joint, parallel-guiding mechanism [18], or parallelogram. Indeed, the flexible mechanism has the shape of a parallelogram, as can be seen from Fig. 5(a), and allows only for translation in one direction. Arai et al. proposed a slightly different version of the compliant Π-joint—see Fig. 5(b)—which uses *notched* beams rather than beams with constant cross-sections. The advantage of the notched Π-joint is higher ratios between the stiffness in the flexible direction and the stiffness in the other directions. The main drawbacks, as pointed out in [19], are smaller beam minimum thickness—thereby rendering machining costlier, while giving rise to higher stress concentration, and leading to limited range of motion.

A. Compliant Realization of the 1D-$2\Pi\Pi\Pi$ *Architecture*

Upon assembling two notched Π joints in series and in the same plane, we obtain a compliant version of the legs

[2]In the sequel, the R joints of the $R\Pi\Pi\Pi R$ chain are not to be confused with those of the parallelograms. We need not refer to the latter as stand-alone joints in this paper

[3]By this term we mean isotropy under *kinetostatic*, *elastostatic*, and *elastodynamic* conditions

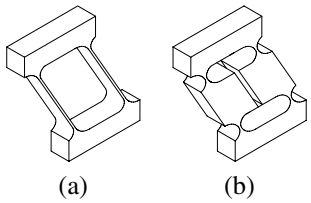

Fig. 5. Compliant realization of the Π-joint (a) with a pair of constant cross-section beams; and (b) with four notched beams

of the 1D-2ΠΠ architecture. We oppose two of these legs to suspend the proof-mass, while orienting them so that their respective planes of motion are orthogonal. The result, as shown in Fig. 6, is a mechanism which is highly stiff in the plane normal to the sensitive axis, and compliant in the direction of that axis.

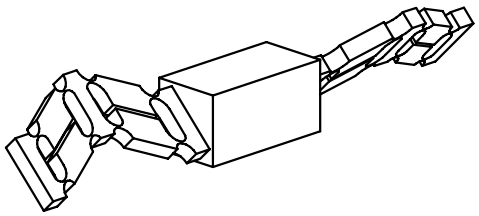

Fig. 6. CAD model of a compliant realization of the 1D-2ΠΠ mechanism

B. Compliant Realization of the 2D-3ΠΠ Architecture

Because of its planar nature, the 2D-3ΠΠ architecture can be realized by means of microfabrication techniques. Here, the type of Π joint could be any of the two proposed in Fig. 5. However, in order to minimize the cross-axis sensitivity, we must keep the out-of-plane thickness as high as possible. There are not many ways, in micromachining, to achieve high thickness-to-width ratios, that is, etch deeper than wide in the substrate. Deep Reactive Ion Etching (DRIE) is probably the most reliable technique, as it allows for trenches of a few microns wide by several hundred microns deep. As a general rule, the etch depth is increased at the expense of the in-plane accuracy, and, for that reason, it is preferable to keep the flexible beams as thick as possible. This leads to the use of constant cross-section beams in the Π joints instead of notched beams.

A CAD model of the corresponding compliant realization of the 2D-3ΠΠ architecture is shown in Fig. 7, a prototype of which is under fabrication at the McGill Nanotools Facility. One may notice that the first Π joint of each leg, that is, the Π joint attached to the accelerometer frame, was mirrored in order to achieve symmetry in each leg. Also, the proof-mass displacements are sensed by measuring the capacitance variations between the electrodes and the proof-mass.

Nevertheless, the proposed architecture lends itself to other types of displacement-measurement techniques, such as piezoresistive and piezoelectric sensing. In those cases, the sensors have to be installed on some of the flexible elements of the mechanism in order to track their angular

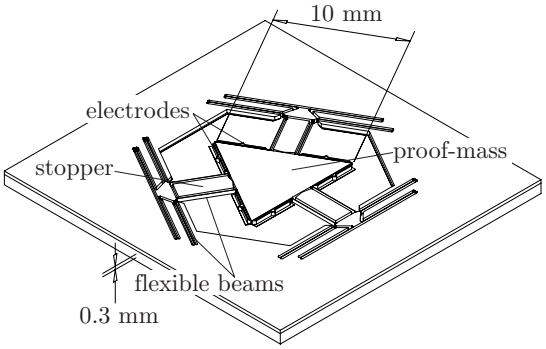

Fig. 7. CAD model of a micromachined compliant realization of the 2D-3ΠΠ mechanism

displacements, and, through a direct kinematics solution, the motion of the proof-mass. An important advantage of the 2D-3ΠΠ architecture is that this problem is linear, provided that the lengths of the intermediate links of the Π joints attached to the proof-mass are known.

To substantiate the above claim, let us label each leg with the subscripts $J = I, II, III$, and sketch the J^{th} leg in an arbitrary posture, as in Fig. 8. Here, we want to

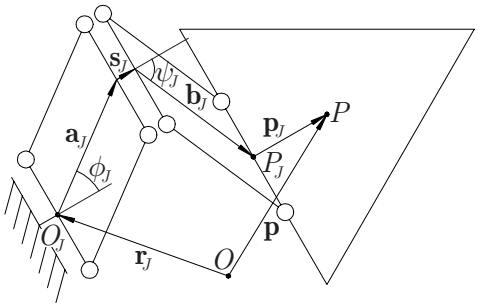

Fig. 8. The J^{th} leg of the 2D-3ΠΠ mechanism

solve for the position vector $\mathbf{p}$ of point P. It is assumed that the angles ϕ_J are measured, whereas angles ψ_J are not. Notice that this problem is planar, which allows us to work with two-dimensional vectors. Therefore, we have $\mathbf{r}_J, \mathbf{a}_J, \mathbf{s}_J, \mathbf{b}_J, \mathbf{p}_J, \mathbf{p} \in \mathbb{R}^2$. Here, points O and O_J are attached to the moving body, and hence, vector $\mathbf{r}_J$ has constant components in a frame fixed to the body. As Π joints allow only for translation of the link opposed to the fixed link, vectors $\mathbf{s}_J$ and $\mathbf{p}_J$ are constant in the frame of the moving body. The position vector $\mathbf{p}$ of point P, the centroid of the moving platform, can thus be written as

$$\mathbf{p} = \mathbf{r}_J + \mathbf{a}_J + \mathbf{s}_J + \mathbf{b}_J + \mathbf{p}_J. \tag{1}$$

We assume that all the legs have the same dimensions and that these dimensions are all known. Therefore, $\mathbf{r}_J$, $\mathbf{s}_J$ and $\mathbf{p}_J$ are known, while $\mathbf{a}_J$ can be computed from its magnitude $a \equiv \|\mathbf{a}_J\|_2$, where $\|\cdot\|_2$ denotes the Euclidean norm of $(\cdot)$, and the measured angle ϕ_J. We let $\mathbf{c}_J$ be the sum of all the foregoing vectors, namely,

$$\mathbf{c}_J \equiv \mathbf{r}_J + \mathbf{a}_J + \mathbf{s}_J + \mathbf{p}_J. \tag{2}$$

Hence, upon substituting eq. (2) into eq. (1), we obtain

$$\mathbf{b}_J = \mathbf{p} - \mathbf{c}_J. \tag{3}$$

We now take the square of the Euclidean norm on both sides of eq. (3), which gives

$$b^2 = \left(\mathbf{p}^T - \mathbf{c}_J^T\right)\left(\mathbf{p} - \mathbf{c}_J\right), \quad J = I, II, III, \tag{4}$$

where $b \equiv \|\mathbf{b}_J\|_2$ is known and constant, besides being identical for all three legs. From eq. (4), it is now apparent that the problem consists in finding the intersection point of three circles of radii b and centered at $\mathbf{c}_J$, $J = I, II, III$. To do this, we rewrite eq. (4) as

$$b^2 - \mathbf{p}^T\mathbf{p} = -2\mathbf{c}_J^T\mathbf{p} + c_J^2, \quad J = I, II, III, \tag{5}$$

where $c_J \equiv \|\mathbf{c}_J\|_2$. Then, we cancel the quadratic term $\mathbf{p}^T\mathbf{p}$ by subtracting eq. (5) with $J = III$ from eq. (5) with $J = II$. Similarly, we subtract I from III and II from I, which leaves us with the system of three linear equations in two unknowns

$$\mathbf{N}\mathbf{p} = \mathbf{m}, \tag{6}$$

where

$$\mathbf{N} \equiv \begin{bmatrix} \mathbf{c}_{II}^T - \mathbf{c}_{III}^T \\ \mathbf{c}_{III}^T - \mathbf{c}_I^T \\ \mathbf{c}_I^T - \mathbf{c}_{II}^T \end{bmatrix} \text{ and } \mathbf{m} \equiv \frac{1}{2}\begin{bmatrix} c_{II}^2 - c_{III}^2 \\ c_{III}^2 - c_I^2 \\ c_I^2 - c_{II}^2 \end{bmatrix}.$$

The 3×2 matrix $\mathbf{N}$ bears full rank if and only if points C_I, C_{II} and C_{III}, with position vectors $\mathbf{c}_I$, $\mathbf{c}_{II}$ and $\mathbf{c}_{III}$, respectively, are non-collinear. As stated before, these points are always so in the 2D-3ΠΠΠ mechanism; therefore, the least-square solution of the foregoing system can be computed directly from the left Moore-Penrose generalized inverse of $\mathbf{N}$. Moreover, in the case where points C_I, C_{II} and C_{III} are the vertices of an equilateral triangle—which takes place at the *equilibrium* posture of the mechanism— matrix $\mathbf{N}$ becomes isotropic. An outcome of this is that the foregoing generalized inverse is *proportional* to $\mathbf{N}^T$ the proportionality factor being the square of the double nonsingular value of $\mathbf{N}$. Hence, solving for $\mathbf{p}$ reduces to the multiplication of a 3×2 matrix by a 2-dimensional vector, which involves a rather limited roundoff error. In general, as the mechanism is to remain close to the equilibrium position, $\mathbf{N}$ remains well conditioned, and solving for $\mathbf{p}$ using this method will give reliable results.

C. Compliant Realization of the 3D-4RΠΠΠR Architecture

The legs of the 3D-4RΠΠΠR mechanism are obtained by appending flexible revolutes at both tips of the legs used in Fig. 6. The axes of these revolutes lie in the plane of the ΠΠ chain. Four of these RΠΠΠR legs are used to connect the regular-tetrahedron-shaped proof-mass to its frame. Each leg is oriented so that its plane contains one edge of the regular tetrahedron and is perpendicular to the opposing edge. The compliant realization thus resulting is shown in Fig. 9, whence it is apparent that the mechanism is compliant to any proof-mass translation in space, while being highly stiff to any rotation of the proof-mass with respect to the accelerometer frame.

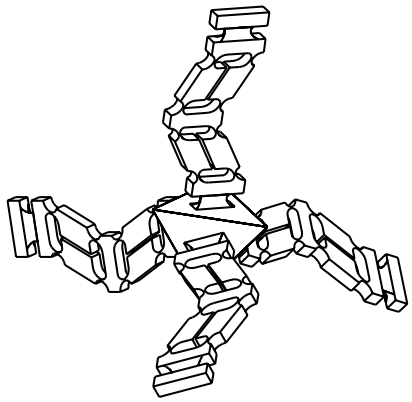

Fig. 9. CAD model of the compliant realization of the 3D-4ΠΠΠ mechanism

Only millimeter-scale models are contemplated for the fabrication of such a mechanism. Indeed, the complicated geometry makes it difficult—if at all possible—to manufacture using existing microfabrication techniques. Hence, for a first prototype, separate machining of the legs and the proof-mass is contemplated. The materials suitable for fabrication are polyurethane, PVC, aluminum and steel. The final selection will depend upon the targeted bandwidth of the accelerometer, its size, and the minimum possible thickness in the flexible beams allowed by the fabrication process.

Also, as it may be difficult or expensive to embed electrodes in this complicated geometry, the contemplated displacement-sensing principles contemplated will rely on piezoresistivity or piezoelectricity. Again, this requires the solution of the direct kinematics problem, which turns out to be nothing but finding the common intersection point of four planes. This problem turns out to be, again, linear. To show this, we label each leg of the three-dimensional 3D-4RΠΠΠR mechanism with the subscripts $J = I, II, III, IV$. Shown in Fig. 10 is a schematic of the simplified kinematic chain of the J^{th} leg. It is assumed that all flexible joints behave like revolutes, which is a good approximation for small displacements of the proof-mass $\mathcal{M}$. We are to find the position vector $\mathbf{p}$ of point P of the moving platform $\mathcal{M}$ from the four measured angles ϕ_J, $J = I, II, III, IV$. The positions of points O_J with respect to point O are known and constant in a body-frame, and so are the positions of points P_J with respect to point P. Apparently, $\mathbf{p}$ can be expressed in terms of all other vectors associated with the J^{th} leg, namely, as

$$\mathbf{p} = \mathbf{r}_J + \mathbf{a}_J + \mathbf{b}_J \tag{7}$$

Also, with angle ϕ_J, it is a simple matter to compute $\mathbf{n}_J$, the unit vector normal to the mid plane of the two Π joints. Since $\mathbf{a}_J$ lies in this plane, it is bound to be orthogonal to

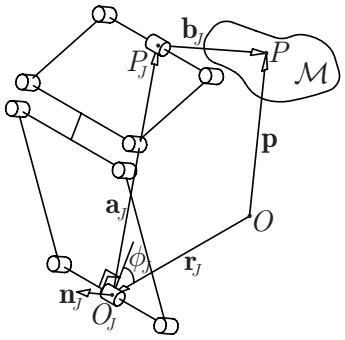

Fig. 10. The J^{th} leg of the 3D-4$R$$\Pi\Pi\Pi$$R$ mechanism

$\mathbf{n}_J$. Hence, we can eliminate $\mathbf{a}_J$ from eq. (7) by multiplying each side by $\mathbf{n}_J^T$ from the left:

$$\mathbf{n}_J^T \mathbf{p} = \mathbf{n}_J^T \left(\mathbf{r}_J + \mathbf{b}_J \right) \tag{8}$$

Writing eq. (8) for all four legs, we obtain a *formally* overdetermined system of four linear equations in three unknowns, the components of $\mathbf{p}$:

$$\mathbf{N}\mathbf{p} = \mathbf{m}, \tag{9}$$

where

$$\mathbf{N} \equiv \begin{bmatrix} \mathbf{n}_I^T \\ \mathbf{n}_{II}^T \\ \mathbf{n}_{III}^T \\ \mathbf{n}_{IV}^T \end{bmatrix}, \text{ and } \mathbf{m} \equiv \begin{bmatrix} \mathbf{n}_I^T (\mathbf{r}_I + \mathbf{b}_I) \\ \mathbf{n}_{II}^T (\mathbf{r}_{II} + \mathbf{b}_{II}) \\ \mathbf{n}_{III}^T (\mathbf{r}_{III} + \mathbf{b}_{III}) \\ \mathbf{n}_{IV}^T (\mathbf{r}_{IV} + \mathbf{b}_{IV}) \end{bmatrix}.$$

Provided that vectors $\mathbf{n}_J$, $J = I, II, III, IV$ are not coplanar, which they are not because of the geometry of the regular tetrahedron, we can find the least-square solution robustly, using an orthogonalization procedure, such as Householder reflections [20].

IV. CONCLUSIONS

A new class of mechanical architectures for multi-axial accelerometers was proposed in order to achieve better cross-axis sensitivity of the sensors. We call these new architectures *simplectic* because they all use one more leg than required by the number of components of the point-acceleration they are meant to measure. Hence, the idea behind these architectures is to arrange the legs normally to each *face* of the simplex corresponding to the dimension of the space of motions generated by the mechanism. The legs are to have just enough mobility to allow the mechanism to span that space, which is achieved by means of compliant revolutes and Π joints. It is shown that the direct kinematics problems associated with the architectures proposed for measuring two and three components of point-acceleration are linear. This simplifies the proof-mass displacements estimation from deflection measurements taken at the revolute joints connecting the mechanism to the accelerometer frame. Indeed, the kinematics problems being linear obviates resorting to any linearization, thereby easing the real-time computations.

V. ACKNOWLEDGMENTS

The support of both NSERC, through a Canada Graduate Scholarship awarded to the first author, and FQRNT, through Research Grant PR-112531, are dutifully acknowledged. The authors are also thankful for the valuable advice on the design of the micromachined biaxial accelerometer provided by Professor Srikar Vengallatore, Dr. Matthieu Nannini, and Mr. Vito Logiudice from the McGill Nanotools Microfabrication Facility.

REFERENCES

[1] B. Barshan and H. F. Durrant-Whyte. Inertial navigation systems for mobile robots. *IEEE Transactions on Robotics and Automation*, 11(3):328–342, 1995.

[2] N. Barbour and G. Schmidt. Inertial sensor technology trends. *IEEE Sensors Journal*, 1(4):332–339, 2001.

[3] M. Elwenspoek and R. Wiergerink. *Mechanical Microsensors*. Springer, New York, USA, 2001.

[4] T. Mineta, S. Kobayashi, Y. Watanabe, S. Kanauchi, I. Nakagawa, E. Suganuma, and M. Esashi. Three-axis capacitive accelerometer with uniform axial sensitivities. *Journal of Micromechanics and Microengineering*, 6:431–435, 1996.

[5] R. Puers and S. Reyntjens. Design and processing experiments of a new miniaturized capacitive triaxial accelerometer. *Sensors and Actuators A*, 68:324–328, 1998.

[6] G. Li, Z. Li, C. Wang, Y. Hao, T. Li, D. Zhang, and G. Wu. Design and fabrication of a highly symmetrical capacitive triaxial accelerometer. *Journal of Micromechanics and Microengineering*, 11:48–54, 2001.

[7] H. C. Kim, S. Seok, I. Kim, S.-D. Choi, and K. Chun. Inertial-grade out-of-plane and in-plane differential resonant silicon accelerometers (drxls). In *IEEE 13th International Conference on Solid-State Sensors, Actuators and Microsystems*, pages 172–175, Seoul, Korea, 2005.

[8] D. Gendre, V. Josselin, and S. Dussy. High-performance accelerometer for on-orbit spacecraft autonomy. In *AIAA Guidance, Navigation, and Control Conference and Exhibit*, pages 3565–3575, Providence, RI, USA, 2004.

[9] F. S. Hillier and G. J. Lieberman. *Introduction to Mathematical Programming*. McGraw–Hill, New York, USA, 1995.

[10] J. M. Hervé. Analyse structurelle des mécanismes par groupes de déplacements. *Mechanism and Machine Theory*, 13, 1978.

[11] J. Angeles. The degree of freedom of parallel robots: A group-theoretic approach. In *Proceedings of IEEE ICRA*, pages 1005–1012, Barcelona, Spain, 2005.

[12] J. M. Hervé and F. Sparacino. Star, a new concept in robotics. In *Proceedings of the 3rd International Workshop on Advances in Robot Kinematics*, pages 176–183, Ferrara, Italy, 1992.

[13] T. Arai, J. M. Hervé, and T. Tanikawa. Development of 3 dof micro finger. In *Proceedings of IROS*, pages 981–987, Osaka, Japan, 1996.

[14] B.-J. Yi, H.-Y. Na, G. B. Chung, W. K. Kim, and I. H. Suh. Design and experiment of a 3dof parallel micro-mechanism utilizing flexure hinges. In *Proceedings of IEEE ICRA*, pages 1167–1172, Washington, DC, USA, 2002.

[15] R. Clavel. Delta, a fast robot with parallel geometry. In *Proceedings of the 18th International Symposium on Industrial Robots*, pages 91–100, Lausanne, Switzerland, 1988.

[16] X. Kong and C. M. Gosselin. Type synthesis of 3-dof translational parallel manipulators based on screw theory. *ASME Journal of Mechanical Design*, 126:83–92, 2004.

[17] H.-H. Pham, I-M. Chen, and H.-C. Yeh. Micro-motion selective actuation xyz flexure parallel mechanism: Design and modeling. *Journal of Micromechatronics*, 3(1):51–73, 2005.

[18] J. M. Derderian, L. L. Howell, M. D. Murphy, S. M. Lyon, and S. D. Pack. Compliant parallel-guiding mechanisms. In *Proceedings of the 1996 ASME Design Engineering Technical Conference*, number 96-DETC/MECH-1208, Irvine, CA, USA, 1996.

[19] B. P. Trease, Y.-M. Moon, and S. Kota. Design of large-displacement compliant joints. *Transactions of the ASME*, 127:788–798, 2005.

[20] G. Golub and C. Van Loan. *Matrix Computations*. Johns Hopkins University Press, Baltimore, 1983.